ARTICLES

A Theoretical Method to Analyze Diffusion of Probe Molecules in Nanostructured Fluids by Fluorescence Correlation Spectroscopy

Kazuhiko Seki,*,† Akiko Masuda,‡ Kiminori Ushida,‡ and M. Tachiya†

National Institute of Advanced Industrial Science and Technology (AIST), AIST Tsukuba Central 5, Higashi 1-1-1, Tsukuba, Ibaraki, Japan, 305−8565 and Riken (The Institute of Physical and Chemical Research) 2-1 Hirosawa, Wako, Saitama, 351−0198 Japan

Received: September 6, 2004; In Final Form: December 1, 2004

In this paper, we study the fluorescence fluctuation correlation function in structured fluids where the diffusion coefficients of probe molecules have different values depending on the distance from initial position, and we derive two simple expressions. Both of them reproduce the exact numerical results rather accurately. One of the expressions contains a time-dependent diffusion coefficient and has a clear physical meaning. We show a procedure to analyze experimental data using the time-dependent diffusion coefficient which results from crossover from free diffusion inside a mesh to hindered diffusion through mesh structures.

I. Introduction

Recently, diffusion coefficients of probe molecules in hyaluronan aqueous solution have been investigated over a wide range of time scales by changing the spectroscopic observation time.[1] The observed diffusion coefficients have a distance dependence resulting from characteristic nano-microstructures of hyaluronan solution.[1] Fast diffusion is observed by photochemical quenching measurements over short distances of ∼10 nm, and the value of the diffusion coefficient is almost the same as that in the absence of hyaluronan. Slow diffusion is observed by pulsed-field gradient NMR over long distances, ∼1−40 μm. The slow diffusion coefficients decrease with increasing concentration of hyaluronan according to the well-known exponential scaling law.[1−6] The diffusion coefficients change between these two extremely different length scales. To probe the transport over distances of hundreds of nanometers, Masuda and Ushida are now probing the system by fluorescence correlation spectroscopy.[7,8] Fluorescence correlation spectroscopy observes concentration fluctuations of probe molecules due to translational diffusion or chemical reactions through fluorescent signals.[9−11] Fluorescence correlation spectroscopy has become widely used after significant improvement of the signal-to-noise ratios.[12−15] The theoretical foundation of fluorescence correlation spectroscopy has been established for homogeneous systems.[10,16] However, hyaluronan solution is highly inhomogeneous due to the mesh structure. Strictly speaking, the fluorescence fluctuation correlation function derived for homogeneous systems is not applicable to inhomogeneous systems over the time range which includes the crossover from free diffusion of probe molecules inside the mesh to hindered diffusion through the mesh structure. A multicomponent diffusion model has been proposed for multiphasic fluids[17,18] but not for mesh structures, where the diffusion coefficients change depending on the length scale of transport. In multicomponent fluids, probe molecules do not necessarily diffuse rapidly at short distances, because they may initially be in the phase where molecules diffuse slowly.

In this paper, we study the fluorescence fluctuation correlation function in structured fluids where the diffusion coefficients of probe molecules have different values depending on the distance from initial position,[19,20] and we derive simple expressions. The diffusion coefficient over distances larger than a characteristic length R is different from that over distances shorter than R.[19,20] When the difference between them is small, the fluorescence fluctuation correlation function derived for homogeneous systems can be used to fit the data within experimental accuracy, and effective diffusion coefficients are obtained from fitting. However, when two diffusion coefficients are very different, the fluorescence fluctuation correlation function derived for homogeneous systems is not applicable. In this paper, we calculate effective diffusion coefficients for structured fluids both numerically and analytically. Effective diffusion coefficients are expressed in terms of fast and slow diffusion coefficients and crossover length, R. Therefore, the crossover length can be obtained by fluorescence correlation spectroscopy if two limiting values of diffusion coefficients are already known from other experiments.[1] Our analytical expression, although it is approximate, gives almost identical results to those of exact numerical calculations even when two limiting diffusion coefficients are very different. The numerical results are also well-fitted by assuming fractional Brownian motion of probe molecules. This means that our theory provides an underlying physical picture for the kinetics described phenomenologically by fractional Brownian motion. Although our work is motivated by experiments on hyaluronan solution, our results are applicable to other systems exhibiting restricted long-range lateral diffusion. For example, generalization of our approach to two-dimensional

† National Institute of Advanced Industrial Science and Technology (AIST).
‡ Riken (The Institute of Physical and Chemical Research).

10.1021/jp045997x CCC: $30.25
Published on Web 03/02/2005

diffusion can be considered as a model of restricted diffusion of probe molecules in membranes.

In section II, we summarize the theoretical basis of fluorescence correlation spectroscopy. Our description of diffusion in inhomogeneous media is introduced in section III. In section IV, results are presented, and in section V, they are used to analyze experimental data. Section VI is devoted to the conclusion.

II. Normalized Autocorrelation Function

In fluorescence correlation spectroscopy, fluctuations of the fluorescence signal stem from changes in the number of fluorescence particles in a confocal laser spot with an intensity profile approximated by a three-dimensional Gaussian function[9−15]

$$I(\vec{r}) = I_0 \exp\left(-\frac{2(x^2+y^2)}{w^2} - \frac{2z^2}{{z_0}^2}\right) \tag{1}$$

where z_0/w is typically in the range ∼5−10. Kinetics of the fluorescence fluctuations is analyzed by the normalized autocorrelation function[9−15]

$$G(\tau) = \frac{\int \mathrm{d}\vec{r}_1 \int \mathrm{d}\vec{r}_0\, I(\vec{r}_1)\, I(\vec{r}_0)\, g(\vec{r}_1 - \vec{r}_0, \tau)}{\int \mathrm{d}\vec{r}\, I(\vec{r})^2} \tag{2}$$

where $g(\vec{r}_1 - \vec{r}_0, \tau)$ is the probability of finding a probe molecule at time τ at position $\vec{r}_1 - \vec{r}_0$ away from its starting point, which is assumed to be the same as that of finding a probe molecule at position $\vec{r}_1$ when it starts from $\vec{r}_0$. By changing variable $\vec{r} = \vec{r}_1 - \vec{r}_0$, $G(\tau)$ is rewritten as

$$G(\tau) = \frac{\int \mathrm{d}\vec{r} \int \mathrm{d}\vec{r}_0\, I(\vec{r} + \vec{r}_0)\, I(\vec{r}_0)\, g(\vec{r}, \tau)}{\int \mathrm{d}\vec{r}\, I(\vec{r})^2}$$

$$= \int \mathrm{d}\vec{r} \exp\left(-\frac{x^2+y^2}{w^2} - \frac{z^2}{{z_0}^2}\right) g(\vec{r}, \tau) \tag{3}$$

where the last equality is obtained by inserting eq 1 into the right-hand side of the first equality and performing Gaussian integrations in the numerator and denominator. In this paper, we focus our attention on the change of $g(\vec{r}, \tau)$ due to lateral diffusion and neglect the changes due to other effects such as reactions and convective transports.[15] When the system is described by uniform media with a diffusion coefficient D_{eff}, $g(\vec{r}, \tau)$ is given by[10]

$$g(\vec{r}, \tau) = \frac{1}{(4\pi D_{\mathrm{eff}}\tau)^{3/2}} \exp\left(-\frac{r^2}{4D_{\mathrm{eff}}\tau}\right) \tag{4}$$

By substituting eq 4 into eq 3, the normalized autocorrelation function is obtained as[10,16]

$$G(\tau) = \frac{1}{1 + 4D_{\mathrm{eff}}\tau/w^2} \frac{1}{\sqrt{1 + 4D_{\mathrm{eff}}\tau/{z_0}^2}} \tag{5}$$

Strictly speaking, eq 5 is not applicable for inhomogeneous fluids. In the following, we calculate the normalized autocorrelation function on the basis of a model of inhomogeneous fluids introduced previously.[19,20]

III. Diffusion in Structured Fluids

Polymer gels have network structures which hinder diffusion over large distances. A theoretical description of the diffusion of probe molecules in polymer gels has been introduced previously to analyze the kinetics observed by fluorescence quenching techniques and NMR.[19,20] In this model, probe molecules diffuse with a diffusion coefficient D_0 inside the sphere of radius R from its initial position and with a diffusion coefficient D_e outside the sphere, as schematically shown in Figure 1. If we denote the probability of finding a probe at time τ at $\vec{r}$ from its initial position by $g_0(\vec{r}, \tau)$ for $r \le R$ and $g_e(\vec{r}, \tau)$ for $r \ge R$, they are Green's functions of the following diffusion equations

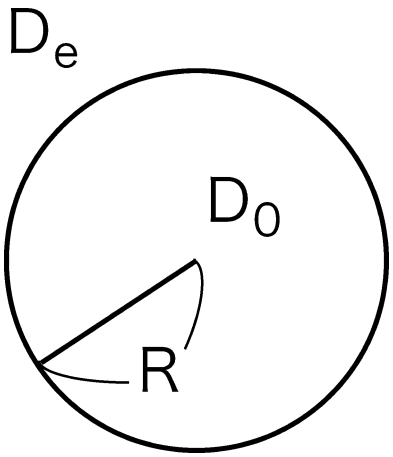

Figure 1. Schematic representation of the model.

$$\begin{cases} \dfrac{\partial}{\partial\tau} g_0(\vec{r}, \tau) = D_0 \nabla^2 g_0(\vec{r}, \tau) \\ \dfrac{\partial}{\partial\tau} g_e(\vec{r}, \tau) = D_e \nabla^2 g_e(\vec{r}, \tau) \end{cases} \tag{6}$$

with the initial condition $g_e(\vec{r}, \tau) = 0$ and

$$g_0(\vec{r}, \tau) = \delta(\vec{r}) \tag{7}$$

The appropriate boundary conditions are $\lim_{r\to\infty} g_e(\vec{r}, \tau) = 0$ and the continuity and flux balance at the boundary[19,20]

$$g_0(\vec{r}, \tau)|_{r=R} = g_e(\vec{r}, \tau)|_{r=R} \tag{8}$$

$$D_0 \frac{\partial}{\partial r} g_0(\vec{r}, \tau)|_{r=R} = D_e \frac{\partial}{\partial r} g_e(\vec{r}, \tau)|_{r=R} \tag{9}$$

We introduce $g^\infty(\vec{r}, \tau)$, Green's function for $R \to \infty$

$$g^\infty(\vec{r}, \tau) = \frac{1}{(4\pi D_0\tau)^{3/2}} \exp\left(-\frac{r^2}{4D_0\tau}\right) \tag{10}$$

which becomes

$$\hat{g}^\infty(\vec{r}, s) = \frac{1}{4\pi D_0 r} \exp(-r\sqrt{s/D_0}) \tag{11}$$

after Laplace transformation $\hat{g}^\infty(\vec{r}, s) = \int_0^\infty \mathrm{d}\tau \exp(-s\tau)\, g^\infty(\vec{r}, \tau)$. Because the solution should be finite at $r \to 0$ and $r \to \infty$, Green's functions in the Laplace domain are given by[19−21]

$$\hat{g}_0(\vec{r}, s) = \hat{g}^\infty(\vec{r}, s) + \frac{C_0(s)}{2\pi D_0 r} \sinh(r\sqrt{s/D_0}), \ (r \le R) \tag{12}$$

$$\hat{g}_e(\vec{r}, s) = \frac{C_e(s)}{4\pi D_0 r} \exp(-r\sqrt{s/D_e}), \ (r \ge R) \tag{13}$$

where two unknown coefficients $C_0(s)$ and $C_e(s)$ are to be determined by boundary conditions eqs 8−9. They are obtained as[19,20]

$$C_0(s) = -\frac{1}{\exp(2R\sqrt{s/D_0})\dfrac{E/\sqrt{s} - F_+}{E/\sqrt{s} - F_-} - 1} \tag{14}$$

$$C_e(s) = \frac{2\exp[R\sqrt{s}(1/\sqrt{D_0} + 1/\sqrt{D_e})]}{E/\sqrt{s} - F_-} C_0(s) \tag{15}$$

where

$$E = \frac{\sqrt{D_0}}{R}\left(1 - \frac{D_e}{D_0}\right), F_\pm = \sqrt{\frac{D_e}{D_0}} \pm 1 \tag{16}$$

The Laplace transform of $G(\tau)$ is obtained as the sum of three terms by substituting eqs 12−13 into eq 3

$$\hat{G}(s) = \hat{G}^\infty(s) + \hat{G}_0(s) + \hat{G}_e(s) \tag{17}$$

where

$$\hat{G}_e(s) = \frac{C_e(s)}{D_0}\int_R^\infty \mathrm{d}r\, r \times \exp\left(-r\sqrt{s/D_e} - \frac{r^2}{w^2}\right) {}_1F_1\left[\frac{1}{2}; \frac{3}{2}; \left(\frac{1}{w^2} - \frac{1}{z_0^2}\right)r^2\right]$$

$$\hat{G}_0(s) = \frac{2C_0(s)}{D_0}\int_0^R \mathrm{d}r\, r \sinh(-r\sqrt{s/D_e}) \times \exp\left(-\frac{r^2}{w^2}\right) {}_1F_1\left[\frac{1}{2}; \frac{3}{2}; \left(\frac{1}{w^2} - \frac{1}{z_0^2}\right)r^2\right]$$

$$\hat{G}^\infty(s) = \frac{1}{D_0}\int_0^R \mathrm{d}r\, r \times \exp\left(-r\sqrt{s/D_0} - \frac{r^2}{w^2}\right) {}_1F_1\left[\frac{1}{2}; \frac{3}{2}; \left(\frac{1}{w^2} - \frac{1}{z_0^2}\right)r^2\right]$$

and ${}_1F_1(a, b, x)$ is the Kummer confluent hypergeometric function.[22] The analytical expression for $G^\infty(\tau)$ is obtained by substituting eq 10 into eq 3 as

$$G^\infty(\tau) = \frac{\mathrm{erf}\left(R\sqrt{\dfrac{1}{4D_0\tau} + \dfrac{1}{z_0^2}}\right)}{\left(1 + \dfrac{4D_0\tau}{w^2}\right)\sqrt{1 + \dfrac{4D_0\tau}{z_0^2}}} - \frac{R\exp\left[-\left(\dfrac{1}{4D_0\tau} + \dfrac{1}{w^2}\right)R^2\right]}{\left(1 + \dfrac{4D_0\tau}{w^2}\right)\sqrt{\pi D_0\tau}} {}_1F_1\left[\frac{1}{2}; \frac{3}{2}; \left(\frac{1}{w^2} - \frac{1}{z_0^2}\right)R^2\right] \tag{18}$$

where $\mathrm{erf}(x)$ is the error function defined by $\mathrm{erf}(x) = (2/\sqrt{\pi})\int_0^x \exp(-t^2)\,\mathrm{d}t$.[22] The other two terms, $G_0(\tau)$ and $G_e(\tau)$, are calculated through numerical Laplace inversion by the Stehfest algorithm.[23] The accuracy of the numerical inversion is confirmed by comparison with the numerical integration based on the expressions obtained by analytical continuation, $G_0(\tau) = (1/\pi i)\int_{-\infty}^{\infty} z\,\mathrm{d}z\,\exp(-z^2\tau)G_0(s)|_{\sqrt{s}=-iz}$ and $G_e(\tau) = (1/\pi i)\int_{-\infty}^{\infty} z\,\mathrm{d}z\,\exp(-z^2\tau)G_e(s)|_{\sqrt{s}=-iz}$.

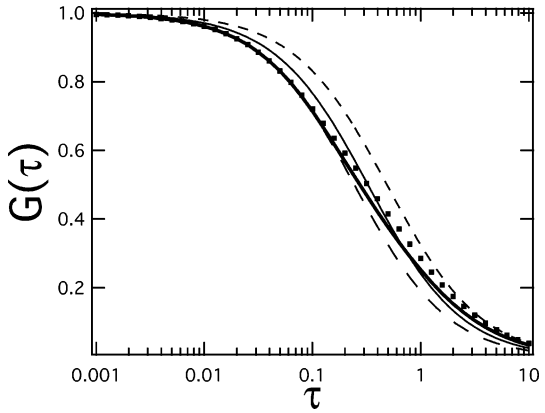

Figure 2. Normalized autocorrelation function as a function of time τ for $R/w = 1.0$, $D_e/D_0 = 0.5$, and $z_0/R = 6.25$. Time is normalized by w^2/D_0. Dots are the exact numerical results. Thick solid line represents the approximate analytical solution, eq 19. Thin solid line is the best fit by eq 5, where $D_{eff}/D_0 = 0.75$. Long dashed line and short dashed line represent eq 5 with $D_{eff} = D_0$ and $D_{eff} = D_e$, respectively.

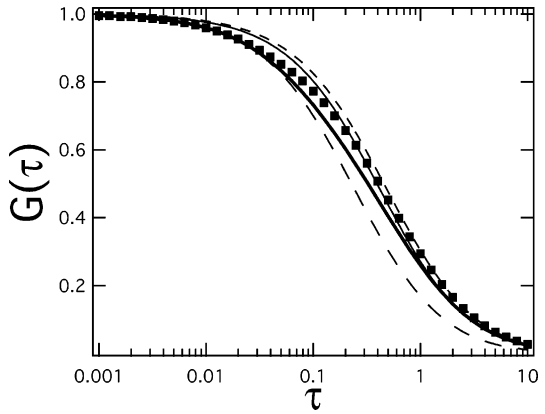

Figure 3. The same as Figure 2 but for $R/w = 0.5$. Thin solid line is the best fit by eq 5, where $D_{eff}/D_0 = 0.58$.

In this model, the diffusion coefficient is small outside the sphere of radius R from the initial position. Length R is introduced to account for hindered diffusion due to the mesh structures of the polymer gels. Although the actual mesh structures of polymer gels may take various forms, it is possible to define the average mesh size. The length R should be related to the average mesh size but is not necessarily the same as it. We will discuss a way to determine R from experimental data later in this paper.

IV. Results

First, we present the results for different values of crossover length R/w and fixed values of parameters $D_e/D_0 = 0.5$, $z_0/R = 6.25$. In Figure 2, R/w is set equal to 1. The exact numerical results are shown by dots. In the same figure, the normalized autocorrelation functions for homogeneous systems, eq 5, with $D_{eff} = D_0$ and $D_{eff} = D_e$ are also presented. The initial decay follows eq 5 with $D_{eff} = D_0$, and the asymptotic decay is described by eq 5 with $D_{eff} = D_e$. The feature remains the same for other values of R/w as shown in Figures 3 and 4 for $R/w = 0.5$ and $R/w = 2.0$, respectively. As the value of R/w is increased, the diffusion of the probe molecules in the laser spot is dominated by the diffusion inside the sphere of radius R, so the time range where the decay is described by eq 5 with D_{eff}

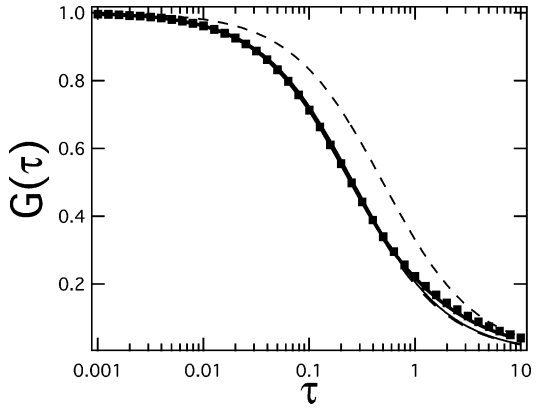

Figure 4. The same as Figure 2 but for $R/w = 2.0$. Thin solid line is the best fit by eq 5, where $D_{eff}/D_0 = 0.95$ and overlaps with long dashed line, $D_{eff}/D_0 = 1.0$.

$= D_0$ increases. On the other hand, as R/w is decreased, the diffusion in the laser spot is dominated by the diffusion outside the sphere of radius R, and the decay is mainly described by eq 5 with $D_{eff} = D_e$.

To construct an approximate analytical solution, we compare three terms, $G^{\infty}(\tau)$, $G_0(\tau)$, and $G_e(\tau)$, in $G(\tau)$. The initial decay is mainly governed by $G^{\infty}(\tau)$, and the asymptotic decay is given by $G_e(\tau)$, and the contribution from $G_0(\tau)$ is negligibly small. Moreover, among the two terms in eq 18, the first term is dominant especially at initial times. Therefore, we obtain an approximate expression

$$G(\tau) = \frac{\mathrm{erf}\left(R\sqrt{\frac{1}{4D_0\tau}+\frac{1}{z_0^2}}\right)}{\left(1+\frac{4D_0\tau}{w^2}\right)\sqrt{1+\frac{4D_0\tau}{z_0^2}}} + \frac{\mathrm{erfc}\left(R\sqrt{\frac{1}{4D_0\tau}+\frac{1}{z_0^2}}\right)}{\left(1+\frac{4D_e\tau}{w^2}\right)\sqrt{1+\frac{4D_e\tau}{z_0^2}}} \quad (19)$$

where $\mathrm{erfc}(x) = 1 - \mathrm{erf}(x)$. Equation 19 is also plotted in Figures 2−4. We can see that eq 19 is an excellent approximation for the exact numerical results. We have confirmed that eq 19 reproduces the exact numerical results very well even when D_e/D_0 is as small as $D_e/D_0 \approx 0.2$.

We can derive another approximate expression for $G(\tau)$. First, we assume that the autocorrelation function for inhomogeneous systems is still given by eq 5 but with a time-dependent D_{eff}, $D_{eff}(\tau)$. Namely,

$$G(\tau) = \frac{1}{1+4\,D_{eff}(\tau)\,\tau/w^2}\,\frac{1}{\sqrt{1+4\,D_{eff}(\tau)\,\tau/{z_0}^2}} \quad (20)$$

Diffusion coefficients should be independent of the parameter z_0, which characterizes the intensity profile of a laser spot. We compare eq 20 with eq 19 in the limit $z_0 \to \infty$. In the long time limit $\tau \to \infty$, the time-dependent diffusion coefficient is obtained as

$$D_{eff}(\tau) = \frac{1}{\frac{\mathrm{erf}(R/\sqrt{4D_0\tau})}{D_0} + \frac{\mathrm{erfc}(R/\sqrt{4D_0\tau})}{D_e}} \quad (21)$$

Equation 20 together with eq 21 gives another approximate expression for $G(\tau)$. The approximate expression is compared with the exact numerical results in Figures 5−7. Equation 20 together with eq 21 reproduces the exact numerical results as

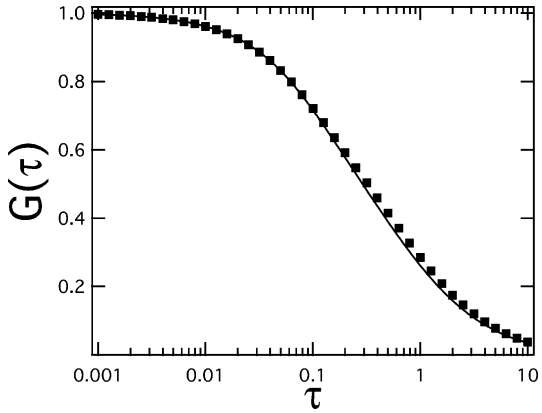

Figure 5. Dots are the same as those in Figure 2. Solid line represents eq 20 with the time-dependent effective diffusion coefficient in eq 21.

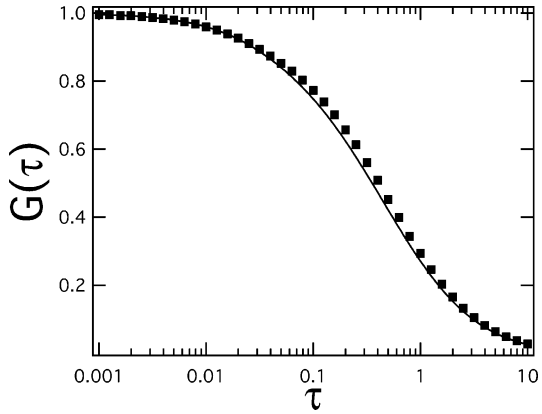

Figure 6. Dots are the same as those in Figure 3. Solid line represents eq 20 with the time-dependent effective diffusion coefficient in eq 21.

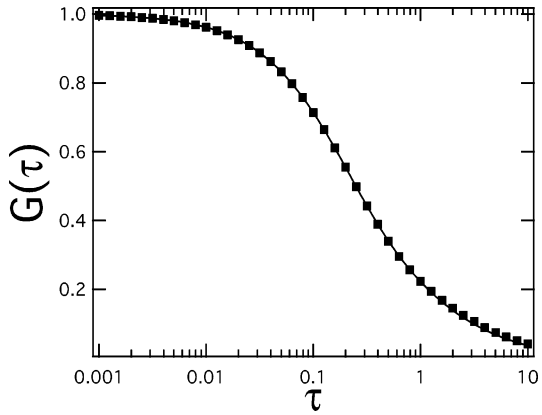

Figure 7. Dots are the same as those in Figure 4. Solid line represents eq 20 with the time-dependent effective diffusion coefficient in eq 21.

accurately as eq 19. The effective time-dependent diffusion coefficient, eq 21, has a clear physical meaning: it is the weighted statistical average of the diffusion coefficients D_0 and D_e, with the weights given by a portion of the probes within the sphere of radius R, $\int_0^{r\le R} \mathrm{d}\vec{r}\; g^{\infty}(\vec{r}, \tau) \approx \mathrm{erf}(R/\sqrt{4D_0\tau})$ for $\tau \to \infty$, and that outside the sphere, $\mathrm{erfc}(R/\sqrt{4D_0\tau}) = 1 - \mathrm{erf}(R/\sqrt{4D_0\tau})$. Equation 20 with eq 21 gives almost identical results to those of the exact numerical calculation, even when D_e is much smaller than D_0, for example, $D_e/D_0 = 0.2$, as shown in Figure 8. When D_e is not much different from D_0, for example, $D_e/D_0 = 0.5$, the expression of the autocorrelation function for homogeneous systems can be used to fit the data within experimental accuracy. The effective diffusion coefficients obtained from fitting are summarized in Figure 9 for

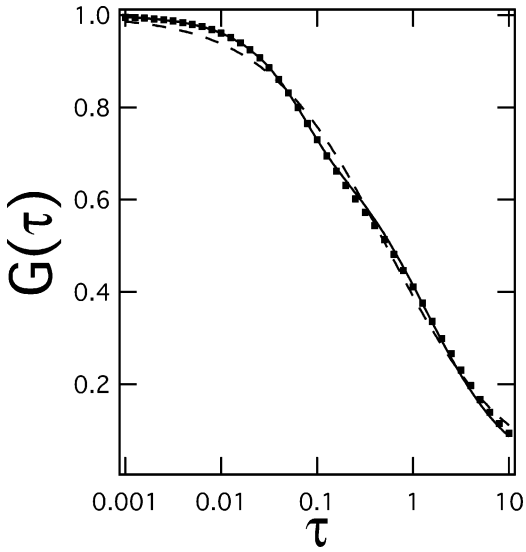

Figure 8. Normalized autocorrelation function as a function of time τ for $D_e/D_0 = 0.2$, $R/w = 1.0$, and $z_0/R = 6.25$. Time is normalized by w^2/D_0. Dots are the exact numerical results. Solid line represents eq 20 with the time-dependent effective diffusion coefficient in eq 21. Dashed line is the best fit by assuming sub-diffusive transport, $\alpha = 0.68$ and $K_\alpha = 0.38$.

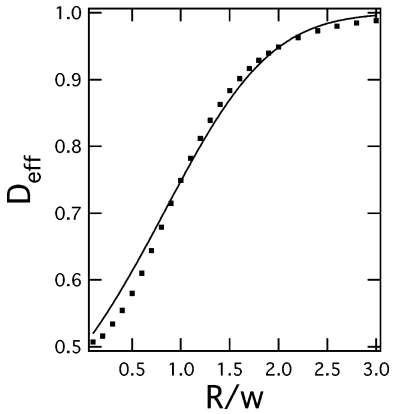

Figure 9. Plot of the effective diffusion coefficient against R/w. Solid line is the approximate expression, $D^*_{\text{eff}} = D_{\text{eff}}(\tau^*)$ given by eq 21 with $\tau^* = 0.54\ w^2/D_0$.

$R/w \approx 0.1-3.0$. We search for an analytical expression of D_{eff} as a function of R/w on the basis of eq 20 together with eq 21. We notice that, if we replace $D_{\text{eff}}(\tau)$ in eq 20 by $D_{\text{eff}}(\tau^*)$, the value of $D_{\text{eff}}(\tau)$ at a certain value (τ^*) of τ, eq 20 is reduced to eq 5 with $D_{\text{eff}} = D_{\text{eff}}(\tau^*)$. If we determine the value of τ^* such that $D_{\text{eff}} = D_{\text{eff}}(\tau^*)$ gives the best fit to the curve of D_{eff} in Figure 9, then $D_{\text{eff}} = D_{\text{eff}}(\tau^*)$ gives an approximate analytical expression of D_{eff} as a function of R/w.

When D_e is much smaller than D_0, the exact numerical result is also fitted very well by assuming fractional Brownian motion of the probe molecules described by $D_{\text{eff}}(\tau) = K_\alpha \tau^{\alpha-1}$ with $\alpha = 0.68$ and $K_\alpha = 0.38$, as shown in Figure 8. If the mean-square displacement of diffusing molecules depends on time as $K_\alpha \tau^\alpha$ for various reasons, then the motion of the particles can be described by fractional Brownian motion. Here, K_α and α are just fitting parameters. These parameters are further related to other physical quantities in some cases. For example, when particles diffuse on fractal structures, α is related to the fractal dimension.[24] Although fractional Brownian motion is frequently observed for hindered diffusion, α is merely a fitting parameter, and its theoretical relation with hindrance has not yet been established.[15,17,25,26] Comparison of the fractional Brownian model with our model shows that the fitting parameters indicate the cross-over length, R, between short-range free diffusion with its coefficient D_0 and long-range hindered diffusion with its coefficient D_e, as well as the ratio between two diffusion coefficients, D_e/D_0. In other words, our theory provides an underlying physical picture for the kinetics phenomenologically described by fractional Brownian motion.

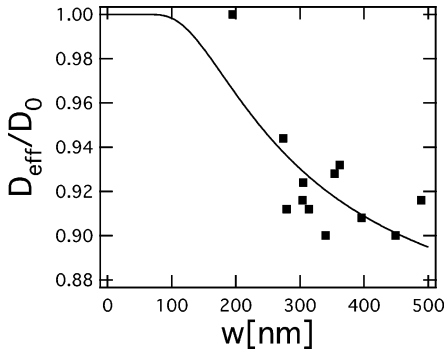

Figure 10. Effective diffusion coefficients of Alexa 488 with 0.1 wt % hyaluronan solution against lateral dimension of laser spot, w. Solid line is the fit by the theoretical expression, $D^*_{\text{eff}} = D_{\text{eff}}(\tau^*)$ given by eq 21 with $\tau^* = 0.54\ w^2/D_0$.

V. Analysis of Experimental Data

We have developed approximate solutions to the model describing hindered diffusion and compared them with numerical results. In this section, we analyze recently observed diffusion coefficients of a fluorescence probe (Alexa Fluor 488) in 0.1 wt % aqueous hyaluronan solution of molecular weight 300 000. Details of the material preparation and the experimental setup have already been described.[8] The observed fluorescence correlation function has been fitted by eq 5 to obtain translational diffusion coefficients, although eq 5 is originally derived by assuming the diffusion of probe molecules in homogeneous solutions. From our model calculations, such an analysis is indeed possible when diffusion coefficients outside the sphere of radius R from its initial position are not so different from those inside the sphere. The observed diffusion coefficients are, however, effective for quantitatively characterizing the diffusional escape of probe molecules from the lateral dimensions of laser spot w. In inhomogeneous systems, the observed effective diffusion coefficients depend on the lateral dimension of laser spot w; the effective diffusion coefficients decrease with increasing w, because the mesh structure of hyaluronan interferes with the lateral diffusion of probe molecules. It is possible to analyze the effective diffusion coefficients thus obtained by our model using $D_{\text{eff}}(\tau^*)$, where $D_{\text{eff}}(\tau)$ is given by eq 21 and $\tau^* = 0.54w^2/D_0$. Strictly speaking, $\tau^* = 0.54w^2/D_0$ is obtained for $D_e/D_0 = {}^1/_2$. We have noticed that τ^* is almost independent of D_e/D_0 when $D_e/D_0 \geq {}^1/_2$. The observed diffusion coefficients of Alexa 488 in 0.1 wt % hyaluronan solution is presented against lateral dimension of laser spot w in Figure 10.

If the value of D_e measured by another experiment is available, the observed effective diffusion coefficient as a function of w is compared to $D_{\text{eff}}(\tau^*)$ obtained from eq 21 with $\tau^* = 0.54w^2/D_0$, where R is an adjustable parameter. The diffusion coefficient at large distances, which corresponds to D_e in our model, is measured by pulsed-field gradient NMR when the probe molecules are cytochrome c. However, D_e is not measured for Alexa 488. Therefore, the observed effective diffusion coefficient is fitted by $D_{\text{eff}}(\tau^*)$ with D_e and R as adjustable parameters. The result with $D_e/D_0 = 0.84$ and $R =$

272 nm is shown in Figure 10. The values are rough estimates, though, because the number of experimental data points is not sufficient to observe any change in effective diffusion coefficients, which would take place around $w \approx 200$ nm. Although the result is preliminary, it suggests that the cross-over length between initial free diffusion and asymptotic hindered diffusion is larger than the average mesh size of the gels. The average mesh size of 33 nm is estimated for 0.1 wt % of hyaluronan (0.65 cm^3/g) by assuming a cubic structure and the radius of chain molecules, 3 Å. The difference in length indicates that probe molecules pass through several regions surrounded by chain molecules until the diffusion is suppressed by obstruction. A similar difference between average mesh size and crossover length of diffusion coefficients is also observed for cytochrome c in 1.5 wt % of hyaluronan, where the average mesh size is estimated to be 5−8 nm, while the crossover length seems to be in the region 10−100 nm, although it is not accessible by experiments at present.[8]

Our theoretical method is useful to extract the cross-over length of the diffusion coefficients from the experimental data. While the average mesh size is a material constant of hyaluronan, the cross-over length of the diffusion coefficients depends both on the concentration of hyaluronan and the size of the probe molecules. The difference in length would be smaller for cytochrome c than for Alexa, because cytochrome c is easily obstructed by hyaluronan molecules by its large size. Further experimental studies by systematically changing the concentration of hyaluronan are needed to find the relation between these length scales.

Masuda and Ushida are now improving the experimental apparatus to make w smaller. They are also planning to perform similar experiments on cytochrome c molecules whose diffusion coefficients are smaller than those of Alexa molecules, and the change in effective diffusion coefficients would be observed at even smaller w. Because D_e of cytochrome c is known from NMR experiments, only the single parameter R is required to fit the observed effective diffusion coefficients against w by $D_{eff}(\tau^*)$. Although our analysis given in this section is far from being complete, our aim is to show a way to analyze experimental data by our theoretical expressions.

VI. Conclusion

The diffusion of probe molecules in structured fluids was investigated by a simple theoretical model introduced previously, where the diffusion coefficient, D_e, of the probe molecules outside the sphere of radius R from its initial position is different from that inside the sphere, D_0. Two approximate expressions are obtained for the normalized fluorescence fluctuation correlation function. Both of them reproduce the exact numerical results accurately for experimentally accessible values of D_0 and D_e. One of the expressions, eq 19, is specific to the quantity observable by fluorescence correlation spectroscopy. The other expression, eq 20, is presented in terms of a time-dependent diffusion coefficient, eq 21. The introduction of a time-dependent diffusion coefficient seems to be useful for analyzing other phenomena involving diffusion. Moreover, as we have shown in the preceding section, the time-dependent diffusion coefficient has a clear physical meaning as the statistical average of slow and fast diffusion coefficients.

The normalized autocorrelation function, eq 5, has been widely used in fluorescence correlation spectroscopy for homogeneous solutions. There are various sources of heterogeneity in biological samples. Only a few analytical expressions of the normalized autocorrelation function have been applied in fluorescence correlation spectroscopy for inhomogeneous systems. One is a multicomponent diffusion model derived for multiphasic fluids. In this model, probe molecules diffuse slowly even at short times when they are in the phase of high viscosity. Obviously hindered diffusion is beyond the scope of applicability of the model, because such slow initial diffusion is very different from the case where molecules diffuse freely inside a mesh until they are obstructed by the mesh structures. Our model takes into account such a cross-over of diffusion coefficients depending on the length scale of transport and is simple enough to derive approximate analytical expressions for the autocorrelation function. For hindered diffusion, experimental data of fluorescence correlation spectroscopy are sometimes analyzed by assuming fractional Brownian motion.[15,17,25,26] However, one should note that fractional Brownian motion is a phenomenological model, in contrast to our model. Numerical values of the autocorrelation function obtained from our model are also described by fractional Brownian motion when the diffusion coefficient, D_e, is very small compared to that of free diffusion, D_0, as shown in Figure 8. Comparison of the fractional Brownian model with our model shows that the parameters in fractional Brownian motion indicate the cross-over length of hindered diffusion as well as the ratio between the two diffusion coefficients, D_e/D_0.

We propose to analyze the experimental data on the basis of eq 21 by the following procedure: First, the fluorescence correlation function should be measured for various values of the characteristic lateral dimension of the laser spot, w, with the concentration of hyaluronan fixed. For each value of w, we can obtain R by fitting the experimental data to eq 20 together with eq 21 if two limiting values of the diffusion coefficients are already known from other experiments.[1] Our theoretical method is justified if R does not deviate greatly by changing w. There may be a case where the experimental data are analyzed by eq 5, although it is applicable only to a homogeneous solution in the strict sense. In this case, D_{eff} obtained from fitting to the experimental data can be used to estimate R from the theoretical curve given by $D_{eff}(\tau^*)$, because D_{eff}/D_0 is a function of R/w if D_e/D_0 is known. Even if D_e/D_0 is unknown, the experimental data of D_{eff}/D_0 against w can be used to estimate R and D_e/D_0 by fitting to $D_{eff}(\tau^*)$. The experimental data we have analyzed in the previous section correspond to this case, and we have estimated R and D_e/D_0. In either case, we obtain R, which corresponds the mesh structures at one concentration of hyaluronan solution. By repeating the same procedure for various concentration of hyaluronan solution, we can study how R changes by changing the concentration. R should also depend on the molecular size of the solute. Meanwhile, the mean mesh size of the gel can be estimated from the cross-section of the chain molecule and the concentration of hyaluronan if a cubic structure is assumed or from the measurement by an electron spin resonance.[27] It would be very interesting to know how these two lengths are related. The diffusion of a particle in hyaluronan solution has been also investigated by simulations.[28] It is revealed that a change in the diffusion coefficients is extremely difficult to observe within the system size of gels accessible by simulations.[28] The physical mechanism behind hindered diffusion has not yet been clearly understood. Recently, Alexandrakis et al. studied the effect of hyaluronidase treatment on diffusion by a multicomponent fluids model.[18] Our theory is based on an alternative picture of structured fluids and focused on hindered diffusion. The time dependence of the diffusion coefficient, eq 21, can be used to test the validity of this picture.

Acknowledgment. This work was supported by the COE development program of the Ministry of Education, Culture, Sports, Science and Technology (MEXT) of Japan.

References and Notes

(1) Masuda, A.; Ushida, K.; Koshino, H.; Yamashita, K.; Kluge, T. *J. Am. Chem. Soc.* **2001**, *123*, 11468.
(2) Gribbon, P.; Heng, B. C.; Hardingham, T. E. *Biophys. J.* **1999**, *77*, 2210.
(3) De Smedt, S. C.; Lauwers, A.; Demeester, J.; Engelborghs, Y.; De Mey, G.; Du, M. *Macromolecules* **1994**, *27*, 141.
(4) Langevin, D.; Rondelez, F. *Polymer* **1978**, *19*, 875.
(5) Ogston, A. G.; Preston, B. N.; Wells, J. D. *Proc. R. Soc. London A* **1973**, *333*, 297.
(6) Cukier, R. I. *Macromolecules* **1984**, *17*, 252.
(7) Ushida, K.; Masuda, A. *HIKARIKAGAKU (Photochemistry)* **2004**, *35*, 10, in Japanese.
(8) Masuda, A.; Ushida, K.; Nishimura, G.; Kinjyo, M.; Tamura, M.; Koshino, H.; Yamashita, K.; Kluge, T. *J. Chem. Phys.* **2004**, *121*, 10787.
(9) Magde, D.; Elson, E. L.; Webb, W. W. *Phys. Rev. Lett.* **1972**, *29*, 705.
(10) Elson, E. L.; Magde, D. *Biopolymers* **1974**, *13*, 1.
(11) Magde, D.; Elson, E. L.; Webb W. W. *Biopolymers* **1974**, *13*, 29.
(12) Rigler, R.; Widengren, J. *Bioscience* **1990**, *3*, 180.
(13) Rigler, R.; Mets, Ü.; Widengren, J.: Kask, P. *Eur. Biophys. J.* **1993**, *22*, 169.
(14) Mets, Ü.; Rigler, R. *J. Fluoresc.* **1994**, *4*, 259.
(15) Schwille, P. *Cell Biochem. Biophys.* **2001**, *34*, 383.
(16) Aragón, S. R.; Pecora, R. *J. Chem. Phys.* **1976**, *64*, 1791.
(17) Schwille, P.; Haupts, U.; Maiti, S.; Webb, W. W. *Biophys. J.* **1999**, *77*, 2251.
(18) Alexandrakis, G.; Brown, E. B.; Tong, R. T.; McKee, T. D.; Campbell, R. B. *Nat. Med. (NY)* **2004**, *10*, 203.
(19) Barzykin, A. V.; Tachiya, M. *J. Phys. Chem. B* **2001**, *107*, 2953.
(20) Price, W. S.; Barzykin, A. V.; Hayamizu, K.; Tachiya, M. *Biophys. J.* **1998**, *74*, 2259.
(21) Carslaw, H. S.; Jaeger, J. C. *Conduction of Heat in Solids*; Oxford University Press: Oxford, 1959.
(22) Abramowitz, M.; Stegun, I. A. *Handbook of Mathematical Functions*; Dover: New York. 1970.
(23) Stehfest, H. *Commun. ACM* **1970**, *13*, 47 and 624.
(24) Alexander, S.; Orbach, R. *J. Phys., Lett.* **1982**, *43*, L625.
(25) Feder, T. J.; Brust-Mascher, I.; Slattery, J. P.; Baird, B.; Webb, W. W. *Biophys. J.* **1996**, *70*, 2767.
(26) Weiss, M.; Hashimoto, H.; Nilsson, T. *Biophys. J.* **2003**, *84*, 4043.
(27) Shenoy, V.; Rosenblatt, J.; Vincent, J.; Gaigalas, A. *Macromolecules* **1995**, *28*, 525.
(28) Takasu, M.; Tomita, J. In *Proceeding of the 3rd Symposium on Slow Dynamics in Complex Systems*; AIP Conference Proceedings: New York. 2004.